JOURNAL OF VIROLOGY, Feb. 2008, p. 1787–1797 Vol. 82, No. 4
0022-538X/08/$08.00+0 doi:10.1128/JVI.01798-07

Cooperative Effect of the Attenuation Determinants Derived from Poliovirus Sabin 1 Strain Is Essential for Attenuation of Enterovirus 71 in the NOD/SCID Mouse Infection Model▽

Minetaro Arita,[1]* Yasushi Ami,[2] Takaji Wakita,[1] and Hiroyuki Shimizu[1]

Department of Virology II[1] and Division of Experimental Animals Research,[2] National Institute of Infectious Diseases, 4-7-1 Gakuen, Musashimurayama-shi, Tokyo 208-0011, Japan

Received 16 August 2007/Accepted 24 November 2007

Enterovirus 71 (EV71) is a causative agent of hand, foot, and mouth disease and is also associated with serious neurological disorders. An attenuated EV71 strain [EV71(S1-3′)] has been established in the cynomolgus monkey infection model; this strain contains the attenuation determinants derived from the type 1 poliovirus vaccine strain, Sabin 1 [PV1(Sabin)], in the 5′ nontranslated region (NTR), 3D polymerase, and 3′ NTR. In this study, we analyzed the effect of the attenuation determinants of PV1(Sabin) on EV71 infection in a NOD/SCID mouse infection model. We isolated a mouse-adapted EV71 strain [EV71(NOD/SCID)] that causes paralysis of the hind limbs in 3- to 4-week-old NOD/SCID mice by adaptation of the virulent EV71(Nagoya) strain in the brains of NOD/SCID mice. A single mutation at nucleotide 2876 that caused an amino acid change in capsid protein VP1 (change of the glycine at position 145 to glutamic acid) was essential for the mouse-adapted phenotype in NOD/SCID mice. Next, we introduced attenuation determinants derived from PV1(Sabin) along with the mouse adaptation mutation into the EV71(Nagoya) genome. In 4-week-old mice, the determinants in the 3D polymerase and 3′ NTR, which are the major temperature-sensitive determinants, had a strong effect on attenuation. In contrast, the effect of individual determinants was weak in 3-week-old NOD/SCID mice, and all the determinants were required for substantial attenuation. These results suggest that a cooperative effect of the attenuation determinants of PV1(Sabin) is essential for attenuated neurovirulence of EV71.

Enterovirus 71 (EV71) is a small nonenveloped virus with a genome of single-strand positive RNA of about 7,500 nucleotides (nt); it belongs to the genus *Enterovirus* of the family *Picornaviridae* (10, 60). EV71 is classified as *Human enterovirus species A*, along with some coxsackie A viruses, such as CA10 and CA16, which cause hand, foot, and mouth disease and herpangina (10, 54). However, EV71 infection is sometimes associated with severe neurological diseases, such as brain stem encephalitis and poliomyelitis-like paralysis (16, 44, 69). Fatal effects of an EV71 outbreak in Taiwan were mostly due to pulmonary edema and/or pulmonary hemorrhage, which may have been caused by direct destruction of the vasomotor and respiratory centers in the brain stem by EV71 infection (11, 23, 25, 36, 40, 70). The case severity rate of EV71 in the outbreak was <0.3% (23). This suggests a high neuropathogenicity of EV71 similar to that of poliovirus (PV), which causes poliomyelitis in 0.1 to 1.0% of infected individuals (reviewed in reference 46). Currently, various vaccines and treatments against EV71 infection are being developed (13, 15, 38, 39, 61, 64, 66, 72, 73).

Experimental infection models of EV71 have been established in the monkey and mouse (14, 21, 22, 49, 50, 71). The advantage of the monkey model is that the monkeys inoculated with clinical isolates of EV71 show neurological disorders similar to those observed in human cases of EV71 infection, including tremor, ataxia, and poliomyelitis-like paralysis; these disorders are critical for the evaluation of the neurovirulence of EV71 strains (3, 5). However, the limited availability of these animals has hampered characterization of the isolates in the monkey infection model. Mouse infection models of EV71 have been established with young mice (1 to 7 days old) (14, 71). For these mouse models, a sufficient number of animals are available, and some clinical symptoms, including rash and paralysis of the hind limbs, were observed in inoculated animals. However, an adaptive mutation(s) of EV71 is required for the infection of mice (14, 71); thus, the model is not useful for the characterization and evaluation of virulence of clinical isolates, but it can be used to evaluate some specific features of EV71 infection (12, 72). The neurological symptoms observed in young mice are difficult to evaluate, in contrast to those observed in adult mice infected with PV (4). Moreover, host range mutations that contribute to attenuation in mice but not in monkeys have been reported for PV (62), suggesting that intrinsic differences in the character of the animals underlie the pathogenesis of enterovirus.

To date, two kinds of mouse models have been established for the analysis of PV infection: one is with transgenic mice (35, 55) which express human PV receptor (34, 45), and another is a surrogate receptor model with nontransgenic mice and PV mutants with a BC loop of type 2 PV Lansing strain, which infects mice via an uncharacterized murine receptor (42, 47). The former mouse model is currently used for the evaluation of the neurovirulence of PV as well as the monkey infection model (48). The latter mouse model was used to de-

* Corresponding author. Mailing address: Department of Virology II, National Institute of Infectious Diseases, 4-7-1 Gakuen, Musashimurayama-shi, Tokyo 208-0011, Japan. Phone: 81-42-561-0771. Fax: 81-42-561-4729. E-mail: minetaro@nih.go.jp.

▽ Published ahead of print on 5 December 2007.

termine the attenuation determinants of PV before the development of the transgenic mouse model (37, 41, 56, 65).

Previously, we used defined genetic manipulation to generate an attenuated strain of EV71 (EV71(S1-3′)] that showed a broad spectrum of antigenicity against EV71 strains with attenuated neurovirulence in cynomolgus monkeys (3, 5). The manipulation was based on the temperature-sensitive determinants of the type 1 PV vaccine strain (Sabin 1) located in the conserved regions of enterovirus genome (58); that is, the 5′ nontranslated region (NTR), 3D polymerase gene, and the 3′ NTR (31, 52, 65). In this manipulation, we focused on the attenuation determinants of Sabin 1 but not those of other vaccine strains (Sabin 2 and Sabin 3 strains) for the following reasons: (i) the attenuation determinant of the Sabin 2 strain was in the capsid proteins but not in the 5′ NTR (57; reviewed by Kew [32]); (ii) the attenuation determinant in the 5′ NTR derived from Sabin 3 strain affected the fitness of the EV71 mutant in vitro (5); and (iii) the Sabin 1 strain has shown a high degree of safety, supported in part by the diverse mechanisms of attenuation with many attenuation determinants throughout the genome (52, 53; reviewed by Minor [46]). EV71(S1-3′) showed limited infection in the central nervous system (CNS), where the virus was isolated only from the spinal cords of inoculated monkeys. The tissue specificity of EV71(S1-3′) was different from that of an EV71 mutant [EV71(3′)] which contained the attenuation determinants in the 3D polymerase gene, and the 3′ NTR, and the virus was isolated from the brain stem and the spinal cord (3, 5), suggesting that a cooperative effect of the introduced mutations is required for limited tissue specificity and attenuated neurovirulence of EV71(S1-3′).

To evaluate the effect of the attenuation determinants derived from the type 1 PV vaccine strain, Sabin 1 [PV1(Sabin)], on the virulence of EV71, we developed an adult mouse infection model of EV71 with nonobese-diabetic–severe combined immunodeficiency (NOD/SCID) mice. It has been known that the appearance of neutralizing antibodies directly correlates with the clearance of coxsackie viruses in a mouse infection model (20) and that innate immunity (alpha/beta interferon response) is critical for restricting the apparent tissue specificity of PV infection (26). Therefore, we used NOD/SCID mice to characterize the effect of attenuation determinants on the tissue specificity of EV71 mutants. NOD/SCID mice have defects in innate immunity derived from the phenotype of NOD mice (depression of natural killer activity, a functional deficit in monocytes to secretes cytokines, and absence of C5 activity of complement), which is associated with decreased resistance to herpes virus infection (7, 29, 68), and also have defects in acquired immunity derived from the phenotype of SCID mice (lack of functional B and T cells) (8, 33). We analyzed tissue specificity and age dependency of EV71 mutants with a mouse adaptation mutation and the attenuation determinants of PV1(Sabin) in the CNSs of NOD/SCID mice.

MATERIALS AND METHODS

Cells and viruses. RD cells (derived from human rhabdomyosarcoma) and 293 cells (derived from human embryonic kidney) (18) were cultured as monolayers in Dulbecco's modified Eagle medium (DMEM) supplemented with 10% fetal calf serum (FCS). For the *trans*-encapsidation of EV71 replicons, 293 cells were cultured in serum-free medium (VP-SFM; Gibco) supplemented with 2% FCS.

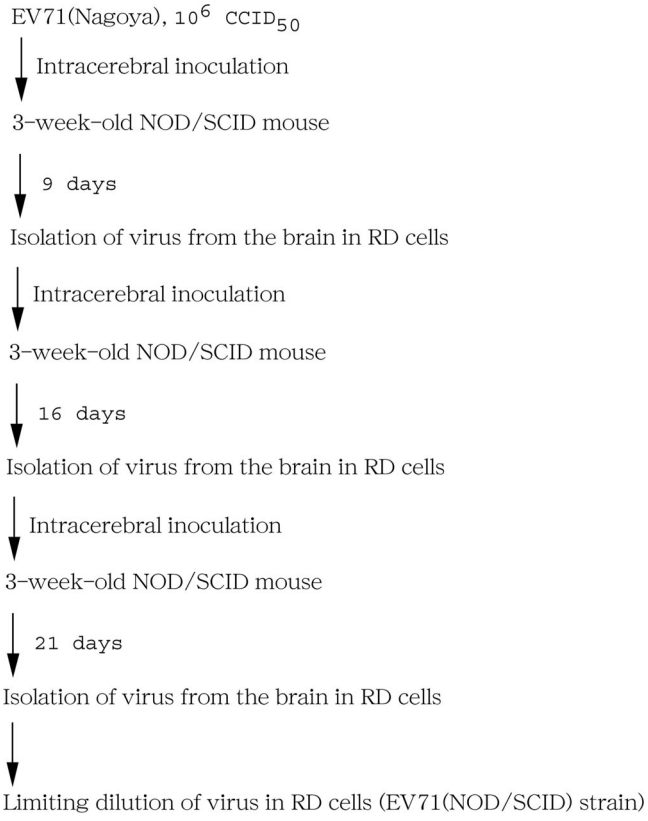

FIG. 1. Adaptation of EV71 in NOD/SCID mice. Three-week-old NOD/SCID mice were inoculated with 10^6 $CCID_{50}$ of EV71(Nagoya) via the intracerebral route. The virus was isolated from the brains of inoculated mice in RD cells. After three rounds of passage, EV71(NOD/SCID) was isolated after limiting dilution in RD cells.

RD cells were used for virus preparation, titration of EV71, and measurement of replication kinetics of EV71 replicon. 293 cells were used for pseudovirus preparation. A mouse-adapted EV71 strain [EV71(NOD/SCID)] was obtained after serial passage of EV71(Nagoya) strain (3, 19) in the brains of NOD/SCID mice (Fig. 1).

General methods of molecular cloning. *Escherichia coli* strain XL10gold (Stratagene) was used for the preparation of plasmids. Ligation of DNA fragments was performed using a quick ligation kit (New England Biolabs). Site-directed mutagenesis (SDM) was performed using KOD Plus DNA polymerase (Toyobo) (59). DNA sequencing was performed using a BigDye Terminator v3.0 cycle sequencing ready reaction kit (Applied Biosystems) and then analyzed with a 3130 genetic analyzer (Applied Biosystems).

Sequence analysis of the genome of the mouse-adapted EV71 strain. The genomic sequence of EV71(NOD/SCID) was determined as described previously (5). Viral genomic RNA was isolated from the culture fluid of infected cells using a High Pure viral RNA kit (Roche). DNA fragments used for DNA sequencing were prepared by reverse transcription-PCR (RT-PCR) using viral genomic RNA as the template by use of a Titan one-tube RT-PCR system (Roche). PCR products were purified using a QIAquick PCR purification kit (Qiagen). The sequences of the 5′ end of the viral genomes were determined using a 5′ rapid-amplification-of-cDNA-ends system, version 2.0 (Invitrogen), according to the manufacturer's instructions. The sequence of the 3′ end of the viral genomes was determined from an RT-PCR product obtained with the primers 7001+ and EcoRI-3END− (Table 1).

Construction of the infectious cDNA clone of mouse-adapted EV71 strains. For the construction of an infectious clone of mouse-adapted EV71 [EV71(NOD/SCID)], a DNA fragment corresponding to nt 1460 to 3444 of EV71(NOD/SCID) was amplified by RT-PCR with the primers *Avr*II-T7-NAGOYA+ and 3602U−. The RT-PCR product was digested by BamHI and NruI and then cloned into the infectious clone of EV71(Nagoya), pEV71(Nagoya) (3). The resultant plasmid was named pEV71(Nagoya-VP231).

TABLE 1. Primers used in this study

Primer	Sequence[a]
2000−	ATTTTACCCGTGGCCATGAATGATC
2876A+	CCCCTACTGGCGAGGTTGTTCCACAATTAC
2876A−	GTAATTGTGGAACAACCTCGCCAGTAGGGG
3164U+	GAACTGTGGGGTCATTGAAATCCAAGTATC
3164U−	GATACTTGGATTTCAATGACCCCACAGTTC
3602U+	GAAGCTAGTGAGTATTTCCCTGCTAGATAC
3602U−	GTATCTAGCAGGGAAATACTCACTAGCTTC
5709+	CGCAACTCTAGTCATCAACACTGAGC
6318A+	GCGCTCTGGGAATCAAAAAAAGAGACATCC
6318A−	GGATGTCTCTTTTTTTGATTCCCAGAGCGC
6399G+	GGGTTGGATCTGCCGTACTCCACTTATG
6399G−	CATAAGTGGAGTACGGCAGATCCAACCC
7001+	GGAGTATGGATTGACCATGACGCCTGCAG
A2*Mlu*I−	AAAAACGCGTTTTTTTTTTTTTTTTTTTTTTTTTTTGCTATTCTGG
AUGSacI+	CACGAAGCGATGGGAGCTCAGGTCTCCAC
AUGSacI−	GTGGAGACCTGAGCTCCCATCGCTTCGTG
*Avr*II-T7-NAGOYA+	TTAACCTAGGTTAATACGACTCACTATAGGTTAAAACAGCCTGTGGGTTGTTCC
dSacI+	GATTGAGAGTTCTATAGGAGATAG
dSacI−	CTATCTCCTATAGAACTCTCAATC
d*Sac*I2+	GTGTGGTTCAGAGCCCTAGAGTTGGTTC
d*Sac*I2−	GAACCAACTCTAGGGCTCTGAACCACAC
EcoRI-3END−	ACTGGAATTCTTTTTTTTTTTTTTTTTTTTTTTTTV
EGFP-Nagoya+	GGGCCTGACCACCTACGGTTCACAAGTGTC
EGFP-Nagoya−	GACACTTGTGAACCGTAGGTGGTCAGGCCC
Fluc-SacI−	ATTGGAGCTCCAATTTGGACTTTCCGCCC
Nagoya-XbaI−	TTAATCTAGATTAAAGAGTAGTGATGGC
SacI-EV3310+	GGCTGAGCTCAGCCGAACGGCAATCACTAC
SacI-Fluc+	TCAGGAGCTCCTGAAGACGCCAAAAAC
XhoI-EGFP+	TGGTCTCGAGACCATGGGAGCTCTGAGC

[a] Variable sequence position in the primer is expressed according to the IUPAC system. Sequences read from the 5′ position at the left end.

Next, a DNA fragment containing the sequence corresponding to nt 1 to 1460 of EV71(NOD/SCID) was obtained by RT-PCR with the primers *Avr*II-T7-NAGOYA+ and 2000−. The RT-PCR product was digested by AvrII and BamHI and then cloned into pEV71(Nagoya-VP231). The resultant plasmid was named pEV71(Nagoya-VP4231). Finally, the mutations of the EV71(NOD/SCID) genome at nt 3602, 6318, and 6399 were introduced into pEV71(Nagoya-VP4231) by serial SDM with primers containing corresponding mutations (3602U+ and 3602U−, 6318A+ and 6318A−, and 6399G+ and 6399G−, respectively). The resultant plasmid was named pEV71(NOD/SCID). To determine the critical mutation for mouse adaptation, we constructed pEV71(Nagoya-VP231-3164U), pEV71(Nagoya-VP23), and pEV71(Nagoya-2876A) by SDM with primer sets containing corresponding mutations (set 3164U+ and 3164U− and set 2876A+ and 2876A−, respectively).

Preparation of EV71 mutants. RNA transcripts of EV71 mutants were obtained using a RiboMAX large-scale RNA production system-T7 kit (Promega) with AvrII-linearized DNA of EV71 infectious clones as the template. RNA transcripts were transfected into a monolayer of RD cells in six-well plates (Falcon) using a Lipofectamine 2000 reagent (Invitrogen), followed by incubation at 37°C in 10% FCS–DMEM (2 ml per well). The cells were harvested when all the cells exhibited the cytopathic effect and were then stored at −70°C. For the binding assay, EV71(Nagoya) and EV71(Nagoya-2876A) were purified as described below.

Construction of EV71 replicon encoding firefly luciferase. For the construction of an EV71 replicon encoding firefly luciferase (EV71-Fluc mc), we removed two SacI sites on the infectious clone of EV71(BrCr-TR) [pEV71(BrCr-TR)] by serial SDM using two primer sets (set d*Sac*I+ and d*Sac*I− and set d*Sac*I2+ and d*Sac*I2−). The resultant plasmid was named pEV71(d*Sac*I′). Next, to remove a SacI site just after the viral genome on the plasmid, a DNA fragment was obtained by PCR using pEV71(BrCr-TR) as the template with primers 5709+ and A2*Mlu*I− and then cloned into pEV71(d*Sac*I′) following digestion by SpeI and MluI. The resultant plasmid was named pEV71(d*Sac*I). Next, a SacI site was introduced just after the initiation codon of the viral protein-coding region of pEV71(d*Sac*I) by SDM with the primers AUG*Sac*I+ and AUG*Sac*I−. To remove the capsid-coding region of the resultant plasmid, PCR was performed with the primers AUG*Sac*I− and *Sac*I-EV3310+ with the resultant plasmid as the template, and then the PCR product was digested by SacI and subjected to self-ligation. The resultant plasmid was named pEV71(d*Sac*I4). Finally, a DNA fragment encoding firefly luciferase was obtained by PCR using pPV-Fluc mc as the template with primers *Sac*I-Fluc+ and Fluc-*Sac*I− (4) and then cloned into pEV71(d*Sac*I4) following digestion by SacI. The resultant plasmid was named pEV71(Fluc-mc).

Construction of EV71 capsid-expressing vectors. For the construction of an expression vector of EV71(Nagoya) capsid proteins, we first fused the enhanced green fluorescence protein (EGFP) gene to the EV71 capsid protein coding region by PCR. The EGFP coding region and the EV71 capsid protein coding region were amplified by PCR with *Xho*I-EGFP+ and EGFP-Nagoya− and with EGFP-Nagoya+ and Nagoya-*Xba*I− using pIRES2-EGFP (Clontech) and pEV71(Nagoya) as templates (3), respectively. Next, these DNA fragments were fused by PCR using the primers *Xho*I-EGFP+ and Nagoya-*Xba*I− and then cloned into the pKS435 expression vector (a kind gift from Koji Sakai, AIDS Research Center, National Institute of Infectious Diseases, Tokyo, Japan), which was useful for the expression of PV capsid proteins (4), following digestion by XhoI and XbaI. The resultant plasmid was named pKS435-EGFP-EV71(Nagoya) capsid. For the analysis of mouse-adapted EV71, a mutation at nt 2876 (change of guanine to adenine) was introduced into pKS435-EGFP-EV71(Nagoya) capsid by SDM with the primers 2876A+ and 2876A−. The resultant plasmid was named pKS435-EGFP-EV71(Nagoya-2876A) capsid. These capsid expression vectors were used for the *trans*-encapsidation of the EV71 replicon.

DNA transfection. A six-well plate (Falcon) with a 30% confluent monolayer of 293 cells was transfected with 1 μg of DNA of pKS435-EGFP-EV71(Nagoya) capsid or pKS435-EGFP-EV71(Nagoya-2876A) capsid per well using a Lipofectamine 2000 reagent (Invitrogen) and then incubated at 37°C in 2 ml per well of 10% FCS–DMEM. The cells were washed with 10% FCS–DMEM at 3 h posttransfection and then used for the *trans*-encapsidation of the EV71 replicon.

***trans*-encapsidation of the EV71 replicon.** For the preparation of *trans*-encapsidated EV71-Fluc mc (TE-EV71-Fluc mc), the RNA transcript of the EV71 replicon was obtained with AvrII-linearized DNA of pEV71-Fluc mc as the template and transfected into a monolayer of 293 cells in six-well plates (Falcon) which transiently expressed EV71 capsid proteins using a Lipofectamine 2000 reagent (Invitrogen), and cells were then incubated at 37°C in 2% FCS–VP-SFM (2 ml per well). The cells were harvested 24 h posttransfection and stored at −70°C.

Virus purification. After freezing and thawing of the harvested cells, EV71 and pseudoviruses were purified from the infected cells using DEAE-Sepharose CL-6B (Amersham Pharmacia Biotech) as described previously (2), followed by centrifugation at 35,000 rpm for 2.5 h at 4°C in a Beckman SW41 rotor with 1 ml of 30% sucrose cushion. The pellet was washed three times with distilled water and then dissolved in 100 μl of phosphate-buffered saline (PBS) with calcium and magnesium (PBS+; 9.6 mM phosphate buffer [pH 7.4], 137 mM NaCl, 2.6 mM KCl, 0.49 mM $MgCl_2$, 0.9 mM $CaCl_2$) at 4°C overnight. The pellet was dissolved by pipetting and then stored at −70°C.

Real-time TaqMan PCR. Real-time TaqMan PCR for the detection of the EV71 genome was performed as previously described by Nijhuis et al. (51). Briefly, viral RNA was isolated from 10% (wt/vol) tissue homogenate in DMEM containing 10% FCS or from serum, which was diluted 1,000-fold with HEPES-buffered saline (HeBS; 21 mM HEPES buffer [pH 7.4], 1.8 mM phosphate, 137 mM NaCl, and 4.8 mM KCl), of infected mice using a High Pure viral RNA purification kit (Roche). The isolated RNA was reverse transcribed using a reverse transcription system (Promega) with random hexamers according to the manufacturer's instructions. The resultant cDNA was assayed in a 20-μl reaction mixture containing 2 μl cDNA solution and 10 μl of TaqMan fast universal PCR master mix (Applied Biosystems) with a forward primer, reverse primer 1, and probe 1 (51). Plasmid DNA of an EV71 infectious clone [pEV71(Nagoya)] was used to control the quantification of the number of copies. The mixtures were subjected to real-time PCR; the PCR conditions consisted of a denaturation step at 95°C for 20 s and 40 cycles of thermal cycling of 95°C for 3 s and 60°C for 30 s. The fluorescence emission of the probe was monitored and analyzed using a 7500 fast real-time PCR system (Applied Biosystems).

Luciferase assay. RD cells in 96-well plates (Falcon) (2.8×10^4 cells per well in 100 μl of Eagle's minimum essential medium supplemented with 2% FCS) were inoculated with 50 μl of the indicated number of copies of TE-EV71(Nagoya)-Fluc mc or TE-EV71(Nagoya-2876A)-Fluc mc and were then incubated at 37°C for 2 h (see Fig. 3C). The cells were washed three times with 10% FCS–DMEM and were then added to 100 μl of 10% FCS–DMEM followed

by incubation at 37°C. The cells were harvested at the indicated times (see Fig. 3C) by adding 30 μl of passive lysis buffer (Promega). Part of the lysate (2 μl) was used for the measurement of luciferase activity. Luciferase activity was measured with a luciferase assay system (Promega) using a TR717 microplate luminometer (Applied Biosystems) according to the manufacturer's instructions.

Electron microscopy. Purified TE-EV71-Fluc mc was subjected to negative staining in uranyl acetate as described previously (67). Samples were examined under transmission electron microscopy (JEM-1220; JEOL Datum) at an acceleration voltage of 80 kV, and the images were obtained at a magnification of ×50,000.

Binding assay. RD cells in 24-well plates (Falcon) (2.2×10^5 cells) were inoculated with 150 μl of 10% FCS–DMEM containing the indicated numbers of copies of purified EV71(Nagoya) or EV71(Nagoya-2876A) in the presence of 2 mM guanidine hydrochloride and were then incubated at room temperature for 30 min (see Fig. 3D). The cells were washed three times with 10% FCS–DMEM and then harvested by adding 100 μl of HeBS containing 2% *N*-lauroylsarcosine. Viral RNA was extracted from the collected cell lysate, and then the number of copies of the viral genome in the cell lysate was determined by real-time TaqMan PCR.

Virus titration. Virus titer was determined by measuring 50% cell culture infective dose ($CCID_{50}$) by microtitration assay in RD cells for EV71 (50) and also by measuring the infectious units (IU) by counting the number of the infected cells stained by the indirect immunofluorescence against firefly luciferase expressed by pseudovirus (4, 6). For the measurement of $CCID_{50}$, virus solution was inoculated into an RD cell suspension on 96-well plates (Falcon) and then incubated at 35°C for 1 week for the observation of cytopathic effect. The $CCID_{50}$ was calculated according to the Behrens-Kärber method (28). For the measurement of IU, pseudovirus solution was diluted with 10% FCS–DMEM and inoculated into RD cell monolayers on 96-well plates (Falcon) (2.8×10^4 cells per well). The cells were incubated at 37°C for 10 h and then fixed with 3% paraformaldehyde. The cells were stained by indirect immunofluorescence with rabbit anti-firefly luciferase antibody (1:100 dilution with 0.1% Triton X-100 in PBS without calcium and magnesium [PBS−]; Cortex Biochem) (1). The number of infected cells was counted for the calculation of IU (27).

Intracerebral inoculation and histological analysis of NOD/SCID mice. All animal procedures were approved by the Committee for Biosafety and Animal Handling and the Committee for Ethical Regulation of the National Institute of Infectious Diseases, Japan. Animal care, breeding, virus inoculation, and observation were performed in accordance with the guidelines of the committees.

NOD/SCID mice (NOD.CB17-*Prkdc*^{scid}/J strain, 3 or 4 weeks old; The Jackson Laboratory) were inoculated with 10^6 $CCID_{50}$ of EV71 mutants via the intracerebral route or with $10^{6.5}$ $CCID_{50}$ of EV71(Nagoya-2876A) via the intravenous route. Inoculated mice were observed for up to 1 month for clinical symptoms (paralysis and death). Mice were sacrificed when paralysis was observed or at 1 month postinoculation (p.i.). For quantification of viral genome in tissues, a portion of excised tissue was stored at −70°C. After freezing and thawing, 10% (wt/vol) tissue homogenates in 10% FCS–DMEM were prepared and centrifuged at $10,000 \times g$ for 10 min to remove cell debris. Supernatants were diluted 10-fold with HeBS and then subjected to RNA extraction. For histological analysis, the tissues of inoculated mice were collected at 4 weeks p.i., and sections of each tissue were prepared. The lesions on the sections were observed after hematoxylin-and-eosin staining. The viral antigen was detected on sections as described previously (48). Sections were deparaffinized with xylene, rehydrated in ethanol, and then treated with 0.25% trypsin solution with 0.5% $CaCl_2$ in PBS− for 30 min and incubated in 1% hydrogen peroxide in methanol to block endogenous peroxidase activity followed by incubation with 10% Block Ace (DS Pharma Biomedical Co., Ltd.) in PBS−. The treated sections were incubated with anti-EV71(C7-Osaka) hyperimmune serum (1:1,000 dilution with 0.1% Triton X-100-PBS−) at 4°C overnight. After three washes with PBS−, the sections were incubated with biotin-conjugated anti-rabbit immunoglobulin G for 30 min at 37°C and then incubated with streptavidin-peroxidase. The peroxidase activity was developed in diaminobenzidine with hydrogen peroxide. The section was counterstained with hematoxylin to stain the nuclei.

Temperature sensitivity. RD cells (1.9×10^5 cells) were inoculated with each virus at a multiplicity of infection of 1 and then incubated at 36°C or at 39°C for 2 h. The cells were washed three times at 2 h p.i., and then 0.5 ml of 10% FCS–DMEM was added to the cells. The cells were incubated at 36°C or at 39°C for 8 h (10 h p.i.) and then stored at −70°C. After freezing and thawing, the viral RNA was extracted from the cell lysate, and then the number of copies of viral RNA was determined using real-time PCR.

RESULTS

Isolation and characterization of a mouse-adapted EV71 strain in NOD/SCID mice. To obtain EV71(NOD/SCID), 3-week-old NOD/SCID mice were inoculated with EV71 (Nagoya) via the intracerebral route, and then the brains were collected and the homogenates were inoculated to RD cells to amplify the virus for the next passage in NOD/SCID mice (Fig. 1). In the third passage, inoculated mice showed paralysis of the hind limbs. Virus was isolated from the paralyzed mice and then purified by limiting dilution in RD cells [EV71(NOD/SCID)]. Sequence analysis of the viral genome showed 16 mutations relative to the parental EV71(Nagoya) genome (Fig. 2A). Among the mutations, one at nt 2876 (a change of guanine to adenine) that caused an amino acid change of glycine to glutamic acid at amino acid position 145 of VP1 capsid protein was sufficient to confer the mouse-adapted phenotype on the parental EV71(Nagoya) (Fig. 2).

Mutation at nt 2876 of EV71 affected binding of the virion to RD cells. To characterize the effect of the mutation at nt 2876 on EV71 infection, we analyzed the early steps of the infection (binding and uncoating steps) of EV71 mutant with the mutation in human RD cells, because EV71(NOD/SCID) could not infect mouse L cells (data not shown).

First, we analyzed the uncoating step of the *trans*-encapsidated EV71 replicons, with or without the mutation, at amino acid position 145 of VP1 protein [TE-EV71(2876A)-Fluc mc and TE-EV71-Fluc mc] (Fig. 3). The titer of TE-EV71-Fluc mc was 1.8×10^5 IU per ml, which was about 2 log lower than that of PV pseudovirus (6.3×10^7 IU per ml) (4). After purification of the pseudovirus, the amount of nonencapsidated viral RNA in the sample was negligible ($<1/10^5$ of the amount of *trans*-encapsidated RNA) (Fig. 3A and B). The replication kinetics of the pseudoviruses were similar, and no lag time caused by delayed uncoating was observed (Fig. 3C). However, the infectivity of TE-EV71(2876A)-Fluc mc was 10-fold lower than that of TE-EV71-Fluc mc.

Next, we analyzed the binding of EV71 virions to RD cells. The titer of EV71(Nagoya-2876A), which has a mouse adaptation mutation at nt 2876, was slightly reduced compared with that of the parental EV71(Nagoya) (10^8 $CCID_{50}$/ml and $10^{8.625}$ $CCID_{50}$/ml, respectively). EV71(Nagoya-2876A) showed a markedly decreased level of binding to RD cells (45-fold) compared with the parental EV71(Nagoya).

These results indicated that the mouse adaptation mutation at nt 2876 affected virus binding in RD cells.

Tissue specificity of mouse-adapted EV71 in NOD/SCID mice. We examined the tissue specificity of an EV71 mutant with mouse adaptation mutation [EV71(Nagoya-2876A)] in NOD/SCID mice. We used a real-time TaqMan PCR method for the detection of the viral RNA because the virus titer in the tissue homogenate was not high enough to be detected by microtitration assay (2.5×10^3 [cerebellum] to 3.8×10^4 [heart] copies of viral RNA per $CCID_{50}$). The numbers of copies per $CCID_{50}$ of EV71 mutants prepared as cell lysates were around 10^3 (Table 2). After intracerebral inoculation with EV71(Nagoya-2876A), we detected the viral RNA in the CNS and in serum at 1 week p.i. (Fig. 4A). At 3 to 4 weeks p.i., a high copy number of viral RNA was detected in the heart and the skeletal muscle as well as in the spinal cord. Viral RNA was

(A)

Nucleotide change	Site of mutation	Amino acid change
584 U(Nagoya) to C(NOD/SCID)	5'NTR	-
602 A(Nagoya) to G(NOD/SCID)	5'NTR	-
736 A(Nagoya) to G(NOD/SCID)	5'NTR	-
930 C(Nagoya) to U(NOD/SCID)	VP4	-
1573 U(Nagoya) to C(NOD/SCID)	VP2	-
1662 C(Nagoya) to U(NOD/SCID)	VP2	-
2005 G(Nagoya) to C(NOD/SCID)	VP3	VP3 97:E(Nagoya) to Q(NOD/SCID)
2244 C(Nagoya) to U(NOD/SCID)	VP3	-
2396 G(Nagoya) to A(NOD/SCID)	VP3	VP3 227:R(Nagoya) to K(NOD/SCID)
2416 C(Nagoya) to G(NOD/SCID)	VP3	VP3 234:H(Nagoya) to D(NOD/SCID)
2488 A(Nagoya) to G(NOD/SCID)	VP1	VP1 16:M(Nagoya) to V(NOD/SCID)
2876 G(Nagoya) to A(NOD/SCID)	VP1	VP1 145:G(Nagoya) to E(NOD/SCID)
3164 U(Nagoya) to C(NOD/SCID)	VP1	VP1 241:L(Nagoya) to S(NOD/SCID)
3602 A(Nagoya) to U(NOD/SCID)	2A	2A 90:Y(Nagoya) to F(NOD/SCID)
6318 G(Nagoya) to A(NOD/SCID)	3D	-
6399 A(Nagoya) to G(NOD/SCID)	3D	-

(B)

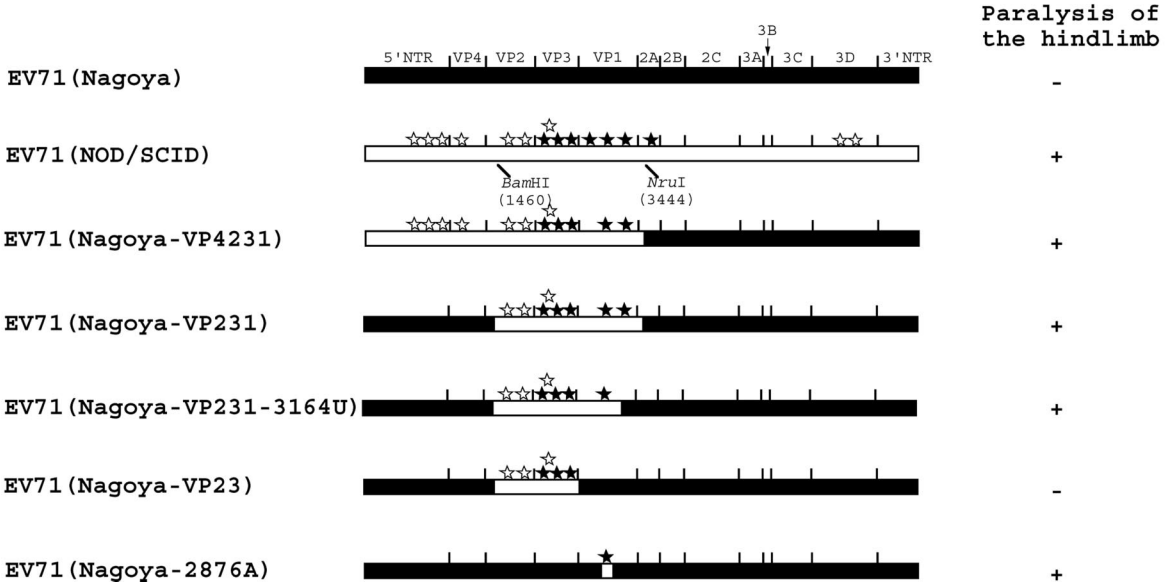

FIG. 2. Identification of the mouse adaptation determinant of EV71(NOD/SCID). (A) Nucleotide and amino acid changes from the parental EV71(Nagoya) to EV71(NOD/SCID). (B) Mouse-adapted phenotypes of EV71 mutants with mouse adaptation mutations. Sequences derived from the parental EV71(Nagoya) genome are represented by the closed regions, and the synonymous and nonsynonymous mutations derived from EV71(NOD/SCID) are represented by the open regions with white and black stars, respectively, above them. + and −, EV71 mutants that did and did not cause paralysis in inoculated mice, respectively.

also detected in other extraneural tissues (lung, liver, spleen, and kidney) along with an increased level of viremia. The preferential virus distribution to the heart observed at 3 and 4 weeks p.i. was also observed at 24 h p.i. after intravenous inoculation (Fig. 4A). The viral antigen was detected only in the heart and the skeletal muscle of inoculated NOD/SCID mice, not in other tissues (Fig. 4B). These results suggest that, along with the CNS, the heart and the skeletal muscle are the major infection sites of a mouse-adapted EV71 strain in NOD/SCID mice.

Effect of attenuation determinants derived from PV1(Sabin) on EV71 infection in NOD/SCID mice. We examined the effects of attenuation determinants derived from PV1(Sabin) on virulence and tissue specificity of EV71(Nagoya-2876A). EV71 mutants containing these determinants showed temperature sensitivity, as previously observed for those constructed based on strain BrCr-TR (5) (Table 3). Minor temperature sensitivity was conferred on the EV71(Nagoya-2876A-S1) mutant by the determinant in the 5′ NTR, and strong temperature sensitivity was conferred on the EV71(Nagoya-2876A-3′) and EV71 (Nagoya-2876A-S1-3′) mutants by the determinants in the 3D polymerase-coding region and in 3′ NTR.

In 3-week-old mice, the effects of individual determinants in the 5′ NTR, 3D polymerase region, and 3′ NTR were weak and could not suppress paralysis in mice inoculated with EV71 mutants (Fig. 5A). However, when all the determinants were introduced into EV71(Nagoya-2876A), the mutant EV71 (Nagoya-2876A-S1-3′) showed drastic reduction in replication (Fig. 5B). The reduction was especially evident in the skeletal muscle and other extraneural tissues, although the levels of

(A)

Pseudovirion	Copy number of viral genomic RNA (in 5 μl)
TE-EV71-Fluc mc	1.2×10^8
TE-EV71(2876A)-Fluc mc	2.5×10^8
EV71-Fluc mc(without capsid)	6.8×10^2

(B)

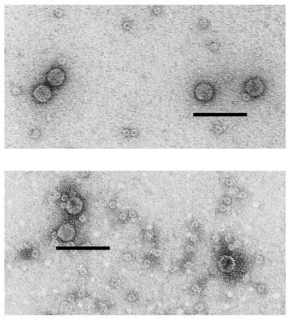

TE-EV71-Fluc mc

TE-EV71(2876A)-Fluc mc

(C)

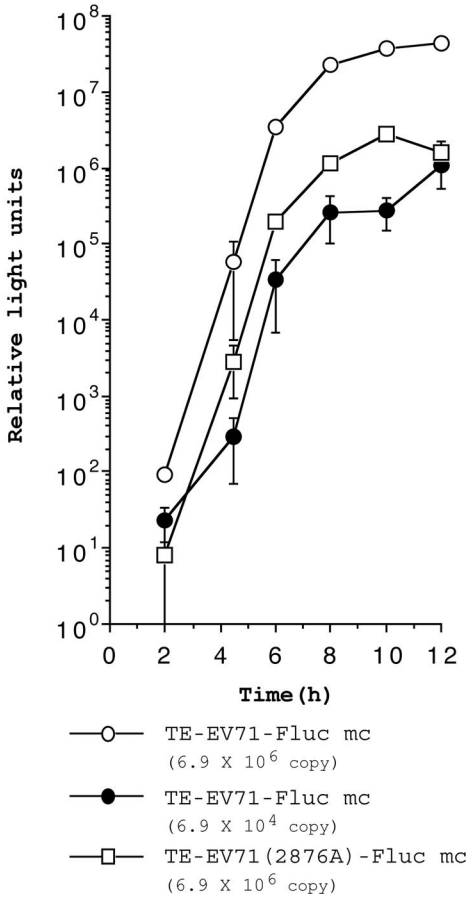

(D)

Virion	Amount of virion added to cells	Amount of virion bound to cells	Binding activity (%)
EV71(Nagoya)	2.1×10^9	$2.9(1.3) \times 10^6$	100
	2.1×10^8	$1.5(0.44) \times 10^5$	100
EV71(Nagoya-2876A)	2.1×10^9	$6.4(1.6) \times 10^4$	2.2
	2.1×10^8	$3.0(1.5) \times 10^3$	2.0

FIG. 3. Effect of mouse adaptation mutation at nt 2876 on EV71 infection in RD cells. (A) Purification of EV71 pseudovirions. The number of copies of viral RNA in purified TE-EV71-Fluc mc and TE-EV71(2876A)-Fluc mc pseudovirions was determined by real-time PCR. The amount of nonencapsidated viral RNA in the sample was determined from samples prepared from 293 cells that were not pretransfected with the DNA of pKS435-EGFP-EV71(Nagoya) capsid vector for capsid proteins expression before RNA transfection with RNA transcript of EV71-Fluc mc. (B) Electron microscopy observation of purified EV71 pseudovirions. Bar, 100 nm. (C) Replication kinetics of EV71 replicon in RD cells infected with pseudovirions. RD cells (1.4×10^4 cells) were infected with 6.9×10^4 to 6.9×10^6 pseudovirions. The cells were washed at 2 h p.i., and then the luciferase activity in the cells was measured at the indicated times. Total luciferase activity with standard deviations is shown. (D) Binding of mouse-adapted EV71 mutant to RD cells. EV71(Nagoya) or EV71(Nagoya-2876A) virions were incubated with RD cells at room temperature for 30 min in the presence of 2 mM guanidine hydrochloride. The amount of virions bound to RD cells was determined by real-time PCR. The binding activity of EV71(Nagoya) was taken as 100%.

viremia were comparable among mice inoculated with the different mutants. Therefore, the cooperative effect of the determinants was critical for the attenuation of EV71 in 3-week-old mice.

TABLE 2. Copy numbers of viral RNA per $CCID_{50}$ of EV71 mutants

EV71 strain	No. of copies of viral genome (in 100 μl)[a]	$CCID_{50}$ (in 100 μl)	No. of copies of viral genome/ $CCID_{50}$
BrCr-TR	3.3×10^9	3.1×10^6	1.1×10^3
Nagoya	3.4×10^9	1.8×10^7	1.9×10^2
Nagoya-2876A	2.0×10^{10}	5.6×10^6	3.6×10^3
Nagoya-2876A-S1	1.7×10^{10}	4.8×10^6	3.5×10^3
Nagoya-2876A-3′	1.8×10^{10}	2.4×10^6	7.5×10^3
Nagoya-2876A-S1-3′	1.4×10^{10}	2.4×10^6	5.8×10^3

[a] Viral RNA was extracted from each virus solution (prepared as crude cell lysates of infected RD cells), and then the number of copies of viral RNA was determined using real-time PCR.

In 4-week-old mice, the effects of individual determinants appeared to be stronger than those observed in 3-week-old mice. Each mutant showed attenuated phenotypes associated with decreased levels of virus replication in the tissues (Fig. 5C). The replication of EV71(2876A-3′) was more severely affected than that of EV71(2876A-S1).

These results suggest that factors required for apparent attenuation depend on the age of the animal and that a cooperative effect of the attenuation determinants is critical for the attenuation of EV71 in NOD/SCID mice.

DISCUSSION

In this study, we established a mouse model of EV71 infection in 3- to 4-week-old NOD/SCID mice with mouse-adapted mutants of EV71(Nagoya). NOD/SCID mice showed a prolonged EV71 infection (>1 month) with broad tissue specificity, possibly supported by the lack of the production of anti-

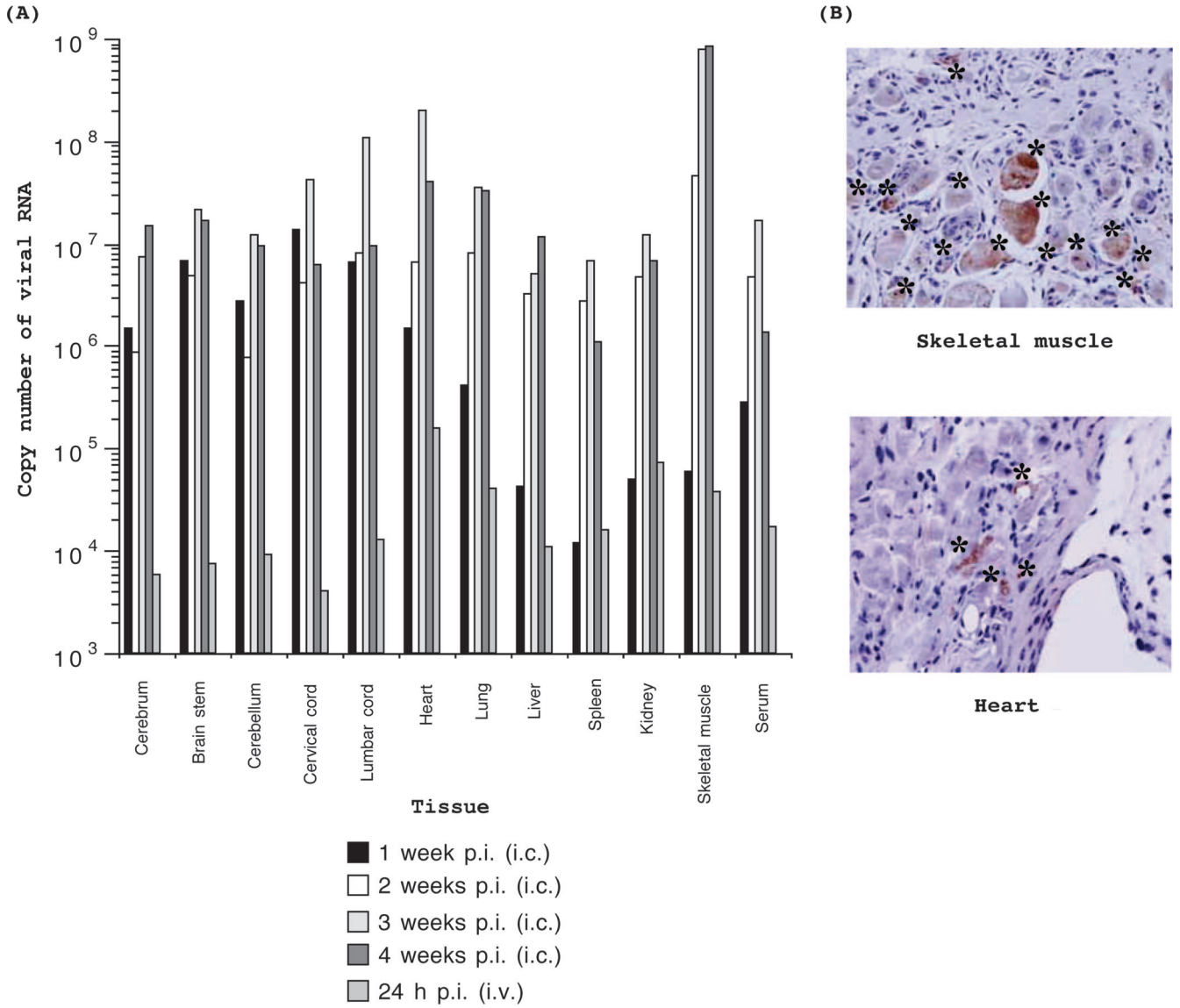

FIG. 4. Infection of NOD/SCID mice with EV71(Nagoya-2876A). (A) Time course of virus dissemination in NOD/SCID mice after intracerebral inoculation. NOD/SCID mice were inoculated with 10^6 $CCID_{50}$ of EV71(Nagoya-2876A) via the intracerebral route, and then the tissues were collected at the time indicated. To determine the primary infection sites after the establishment of viremia, NOD/SCID mice were inoculated with $10^{6.5}$ $CCID_{50}$ of EV71(Nagoya-2876A) via the intravenous route, and then the tissues were collected at 24 h p.i. The number of copies of viral RNA in each tissue was determined by real-time PCR. The number of copies of viral RNA in 0.1 g of each tissue or in 5 μl of serum are shown. (B) Detection of viral antigen in NOD/SCID mice. The viral antigen was detected in the skeletal muscles and hearts of infected mice. The cells with viral antigen are shown with an asterisk.

EV71 antibody in NOD/SCID mice (Fig. 4) (20). The permissive age of NOD/SCID mice for mouse-adapted EV71 infection (>3 weeks old) was higher than the permissive ages of the reported mouse infection models with normal mice (1 to 7 days old) (14, 71). We identified a mutation at nt 2876 that caused a single amino acid change of VP1 at amino acid position 145 as the determinant of mouse adaptation of EV71(Nagoya) (Fig. 2). This amino acid residue is located at around the fivefold axis on the surface of the EV71 virion, according to a structure model calculated from the crystal structure of bovine enterovirus (63). However, mouse-adapted EV71 strains and EV71 pseudoviruses with the mouse adaptation determinant at nt 2876 could not infect mouse L cells. When the in vitro-synthesized RNA transcript of EV71 replicon was transfected into mouse L cells, vigorous replication was observed (M. Arita, unpublished observation). Therefore, it is plausible that isolated mouse-adapted strains could not infect mouse L cells because of the lack of a receptor on the cells. The number of copies of the pseudovirions were similar with and without the mutation at nt 2876, suggesting encapsi-

TABLE 3. Temperature sensitivity of EV71 mutants

EV71 strain	No. of copies		Δ 36/39°C[a]
	36°C	39°C	
Nagoya-2876A	1.6×10^9	1.0×10^9	0.2
Nagoya-2876A-S1	1.1×10^9	3.0×10^8	0.6
Nagoya-2876A-3′	8.3×10^7	2.0×10^5	2.6
Nagoya-2876A-S1-3′	2.1×10^8	8.0×10^4	3.4

[a] Log_{10} ratio of the numbers of copies observed at 36 and 39°C.

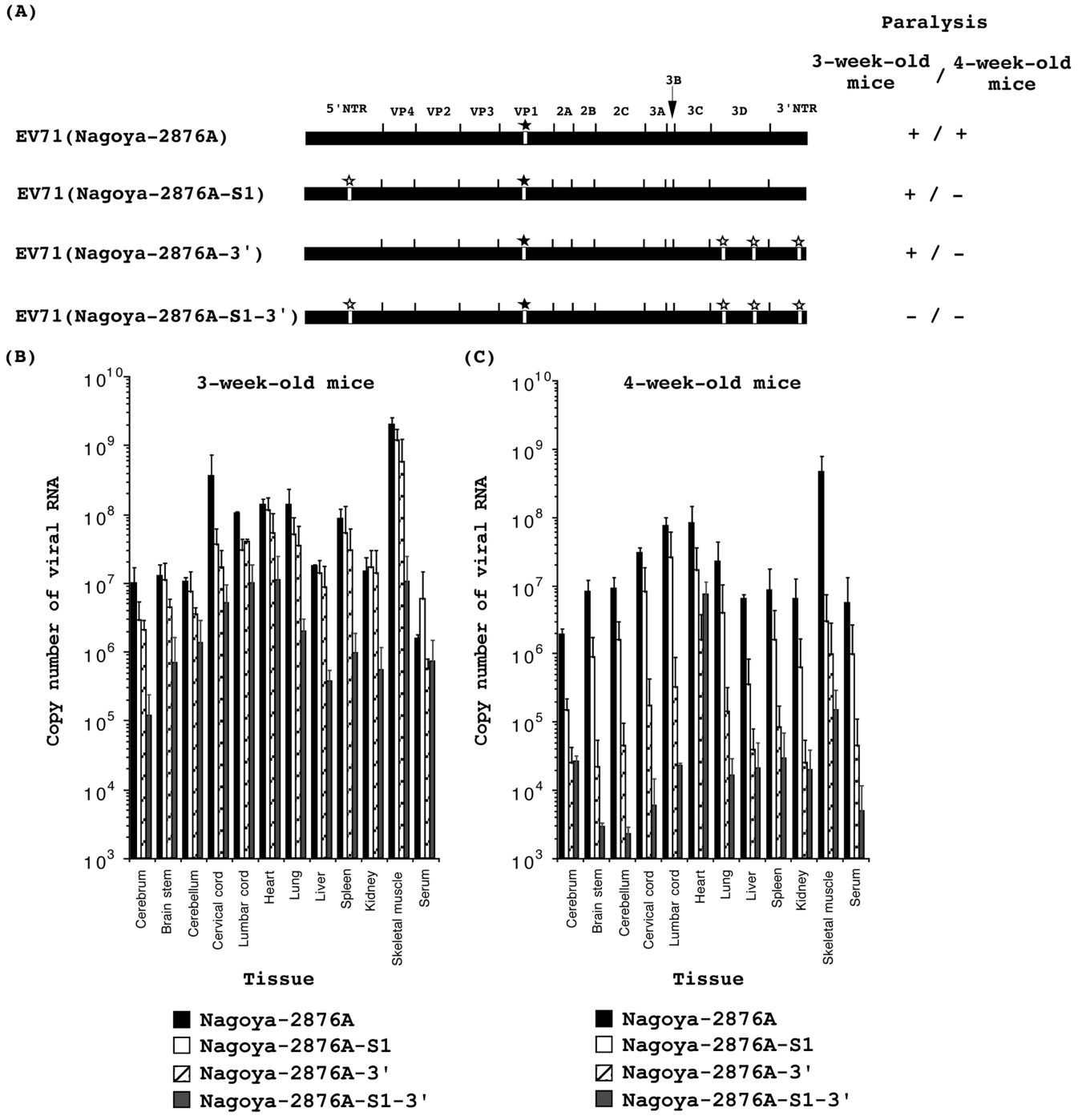

FIG. 5. Characterization of the effect of the attenuation determinants of PV1(Sabin) on EV71 infection in NOD/SCID mice. (A) Mouse-adapted phenotype of EV71(Nagoya-2876A) with the attenuation determinants of PV1(Sabin). The sequences derived from the parental EV71(Nagoya) genome are represented by the closed regions, and the introduced mutations are represented by the open regions with stars above them. White stars represent the attenuation determinants of PV1(Sabin) and black stars represent a mouse adaptation mutation derived from EV71(NOD/SCID) at nt 2876. + and −, EV71 mutants that did and did not cause paralysis, respectively, in the inoculated mice (3 and 4 weeks old). (B and C) Tissue specificity of EV71 mutants in 3- and 4-week-old NOD/SCID mice. NOD/SCID mice were inoculated with 10^6 $CCID_{50}$ of each mutant via the intracerebral route, and the tissues were collected when the mice showed paralysis or at 4 weeks p.i. The number of copies of viral RNA in each tissue was determined by real-time PCR. The number of copies of viral RNA in 0.1 g of each tissue or in 5 μl of serum is shown.

dation was not the target step of the mutation for mouse adaptation (Fig. 3A). The mutation at nt 2876 affected the virion binding (Fig. 3D). The thermostability of EV71(Nagoya-2876A) examined in the range of 37 to 47°C was comparable to that of the parental strain EV71(Nagoya) (data not shown), which is considered important for the mouse adaptation of PV with enhanced uncoating efficiency (17). The mutation at nt 2876 might increase the efficiency of uncoating upon

specific binding of the virion to the receptor molecule on the target cells in NOD/SCID mice, although the increase in the uncoating efficiency observed in human RD cells was at most 4.5-fold (Fig. 3C and D). These observations suggest that the primary effect of the mouse adaptation mutation is on the enhancement of the virion binding to the target cells in NOD/SCID mice to facilitate the infection of the mouse-adapted EV71 strain.

We observed broad tissue specificity of mouse-adapted EV71 in NOD/SCID mice (Fig. 4). The inoculated NOD/SCID mice showed paralysis of the hind limbs at 2 to 4 weeks p.i. but not of the forelimbs, although a similar level of replication was observed in the cervical and the lumbar spinal cords after intracerebral inoculation (Fig. 4 and 5; also data not shown). Among the tissues examined, along with the CNS, the heart and the skeletal muscle were the major targets of EV71 infection in NOD/SCID mice. Abundant viral-antigen-positive cells were observed in the skeletal muscles of the hind limbs, showing atrophic polymyositis with degeneration of the muscle cells and proliferation of fibroblasts in the interstitial tissue, while only a few muscle cells were positive in the heart (Fig. 4A). In contrast, we observed no lesions and no dissolution of neurons in the brain stem and lumbar spinal cord (data not shown). In humans and monkeys, the major infection sites of EV71 were in the brain stem and the spinal cord (3, 40, 49, 50). Therefore, the tissue specificity of a mouse-adapted EV71 strain in NOD/SCID mice was different from specificities in humans and monkeys. Interestingly, the observed tissue specificity of an EV71 mutant with a mouse adaptation determinant [EV71(Nagoya-2876A)] showed a good correlation with the viral internal ribosomal entry site activities in mice (30). This suggests that the tissue specificity of EV71(Nagoya-2876A) was determined after the step of virus binding to the target cells in NOD/SCID mice. The viral antigen was detected in the heart and skeletal muscle but not in the CNS tissues of NOD/SCID mice (Fig. 4B). Muscle tissues are hard to homogenize compared with CNS tissues. Therefore, the virus titer in muscle tissues might have been underestimated by inefficient extraction of the viral RNA from these tissues. In a mouse infection model of EV71 using 7-day-old mice, the muscle contained the highest titer of virus, and the limb muscles displayed massive necrosis from the infection (71). Therefore, the observed paralysis of the hind limbs in NOD/SCID mice might be caused by polymyositis and not by the lesion in the CNS. The target cells of EV71(Nagoya-2876A) in NOD/SCID mice need to be determined in future studies.

A cooperative effect of the attenuation determinants of PV1(Sabin) on the attenuation of PV has been observed in monkey and mouse infection models (9, 24, 43, 52, 65), and in a monkey model of EV71 infection (3, 5). We observed that the cooperative attenuation effect on EV71 infection in NOD/SCID mice was age independent (Fig. 5). However, individual effects of the determinants were age dependent. The determinants of PV1(Sabin) in the 3D polymerase and 3′ NTR, which are known as strong temperature-sensitive determinants (5, 9), conferred an attenuated phenotype on EV71 in 4-week-old mice but not in 3-week-old mice. This suggests that temperature sensitivity could be the dominant factor for attenuation in adult mice. In fact, an attenuation determinant in the 5′ NTR of PV3(Sabin), which served as a major attenuation determinant in adult mice (4 weeks old) but not in newborn mice (1 to 2 days old), has been reported (30). These results indicate that the cooperative effect of the attenuation determinants is critical for the attenuation of EV71 in NOD/SCID mice.

The tissue specificities of EV71 mutants examined in this study were similar in the CNS, suggesting that the introduced determinants had no effect on the tissue specificity of EV71 in the CNS. This suggests that the neuroattenuated phenotype of EV71(S1-3′) in the brain stems of cynomolgus monkeys was conferred by a non-tissue-specific cooperative effect of the determinants.

In summary, we developed an NOD/SCID mouse model of EV71 infection and characterized the effect of the attenuation determinants of PV1(Sabin) on the attenuation of EV71 in NOD/SCID mice. The results suggest that a cooperative effect of attenuation determinants is critical for attenuation of EV71.

ACKNOWLEDGMENTS

We are grateful to Junko Wada for her excellent technical assistance.

This study was supported by Grants-in-Aid from the Japan Society for Promotion of Science and for Research on Emerging and Re-emerging Infectious Diseases from the Ministry of Health, Labor and Welfare.

REFERENCES

1. **Arita, M., H. Horie, M. Arita, and A. Nomoto.** 1999. Interaction of poliovirus with its receptor affords a high level of infectivity to the virion in poliovirus infections mediated by the Fc receptor. J. Virol. **73:**1066–1074.
2. **Arita, M., S. Koike, J. Aoki, H. Horie, and A. Nomoto.** 1998. Interaction of poliovirus with its purified receptor and conformational alteration in the virion. J. Virol. **72:**3578–3586.
3. **Arita, M., N. Nagata, N. Iwata, Y. Ami, Y. Suzaki, K. Mizuta, T. Iwasaki, T. Sata, T. Wakita, and H. Shimizu.** 2007. An attenuated strain of enterovirus 71 belonging to genotype A showed a broad spectrum of antigenicity with attenuated neurovirulence in cynomolgus monkeys. J. Virol. **81:**9386–9395.
4. **Arita, M., N. Nagata, T. Sata, T. Miyamura, and H. Shimizu.** 2006. Quantitative analysis of poliomyelitis-like paralysis in mice induced by a poliovirus replicon. J. Gen. Virol. **87:**3317–3327.
5. **Arita, M., H. Shimizu, N. Nagata, Y. Ami, Y. Suzaki, T. Sata, T. Iwasaki, and T. Miyamura.** 2005. Temperature-sensitive mutants of enterovirus 71 show attenuation in cynomolgus monkeys. J. Gen. Virol. **86:**1391–1401.
6. **Barclay, W., Q. Li, G. Hutchinson, D. Moon, A. Richardson, N. Percy, J. W. Almond, and D. J. Evans.** 1998. Encapsidation studies of poliovirus subgenomic replicons. J. Gen. Virol. **79:**1725–1734.
7. **Baxter, A. G., and A. Cooke.** 1993. Complement lytic activity has no role in the pathogenesis of autoimmune diabetes in NOD mice. Diabetes **42:**1574–1578.
8. **Bosma, G. C., R. P. Custer, and M. J. Bosma.** 1983. A severe combined immunodeficiency mutation in the mouse. Nature **301:**527–530.
9. **Bouchard, M. J., D. H. Lam, and V. R. Racaniello.** 1995. Determinants of attenuation and temperature sensitivity in the type 1 poliovirus Sabin vaccine. J. Virol. **69:**4972–4978.
10. **Brown, B. A., and M. A. Pallansch.** 1995. Complete nucleotide sequence of enterovirus 71 is distinct from poliovirus. Virus Res. **39:**195–205.
11. **Chang, L. Y., T. Y. Lin, K. H. Hsu, Y. C. Huang, K. L. Lin, C. Hsueh, S. R. Shih, H. C. Ning, M. S. Hwang, H. S. Wang, and C. Y. Lee.** 1999. Clinical features and risk factors of pulmonary oedema after enterovirus-71-related hand, foot, and mouth disease. Lancet **354:**1682–1686.
12. **Chen, C. S., Y. C. Yao, S. C. Lin, Y. P. Lee, Y. F. Wang, J. R. Wang, C. C. Liu, H. Y. Lei, and C. K. Yu.** 2007. Retrograde axonal transport: a major transmission route of enterovirus 71 in mice. J. Virol. **81:**8996–9003.
13. **Chen, H. F., M. H. Chang, B. L. Chiang, and S. T. Jeng.** 2006. Oral immunization of mice using transgenic tomato fruit expressing VP1 protein from enterovirus 71. Vaccine **24:**2944–2951.
14. **Chen, Y. C., C. K. Yu, Y. F. Wang, C. C. Liu, I. J. Su, and H. Y. Lei.** 2004. A murine oral enterovirus 71 infection model with central nervous system involvement. J. Gen. Virol. **85:**69–77.
15. **Chiu, C. H., C. Chu, C. C. He, and T. Y. Lin.** 2006. Protection of neonatal mice from lethal enterovirus 71 infection by maternal immunization with attenuated Salmonella enterica serovar Typhimurium expressing VP1 of enterovirus 71. Microbes Infect. **8:**1671–1678.
16. **Chumakov, M., M. Voroshilova, L. Shindarov, I. Lavrova, L. Gracheva, G. Koroleva, S. Vasilenko, I. Brodvarova, M. Nikolova, S. Gyurova, M.**

Gacheva, G. Mitov, N. Ninov, E. Tsylka, I. Robinson, M. Frolova, V. Bashkirtsev, L. Martiyanova, and V. Rodin. 1979. Enterovirus 71 isolated from cases of epidemic poliomyelitis-like disease in Bulgaria. Arch. Virol. **60:**329–340.

17. **Couderc, T., F. Delpeyroux, H. Le Blay, and B. Blondel.** 1996. Mouse adaptation determinants of poliovirus type 1 enhance viral uncoating. J. Virol. **70:**305–312.
18. **Graham, F. L., J. Smiley, W. C. Russell, and R. Nairn.** 1977. Characteristics of a human cell line transformed by DNA from human adenovirus type 5. J. Gen. Virol. **36:**59–74.
19. **Hagiwara, A., I. Tagaya, and T. Yoneyama.** 1978. Epidemic of hand, foot and mouth disease associated with enterovirus 71 infection. Intervirology **9:**60–63.
20. **Harvala, H., H. Kalimo, J. Bergelson, G. Stanway, and T. Hyypia.** 2005. Tissue tropism of recombinant coxsackieviruses in an adult mouse model. J. Gen. Virol. **86:**1897–1907.
21. **Hashimoto, I., and A. Hagiwara.** 1983. Comparative studies on the neurovirulence of temperature-sensitive and temperature-resistant viruses of enterovirus 71 in monkeys. Acta Neuropathol. (Berlin) **60:**266–270.
22. **Hashimoto, I., and A. Hagiwara.** 1982. Pathogenicity of a poliomyelitis-like disease in monkeys infected orally with enterovirus 71: a model for human infection. Neuropathol. Appl. Neurobiol. **8:**149–156.
23. **Ho, M., E. R. Chen, K. H. Hsu, S. J. Twu, K. T. Chen, S. F. Tsai, J. R. Wang, and S. R. Shih.** 1999. An epidemic of enterovirus 71 infection in Taiwan. N. Engl. J. Med. **341:**929–935.
24. **Horie, H., S. Koike, T. Kurata, Y. Sato-Yoshida, I. Ise, Y. Ota, S. Abe, K. Hioki, H. Kato, C. Taya, T. Nomura, S. Hashizume, H. Yonekawa, and A. Nomoto.** 1994. Transgenic mice carrying the human poliovirus receptor: new animal models for study of poliovirus neurovirulence. J. Virol. **68:**681–688.
25. **Huang, C. C., C. C. Liu, Y. C. Chang, C. Y. Chen, S. T. Wang, and T. F. Yeh.** 1999. Neurologic complications in children with enterovirus 71 infection. N. Engl. J. Med. **341:**936–942.
26. **Ida-Hosonuma, M., T. Iwasaki, T. Yoshikawa, N. Nagata, Y. Sato, T. Sata, M. Yoneyama, T. Fujita, C. Taya, H. Yonekawa, and S. Koike.** 2005. The alpha/beta interferon response controls tissue tropism and pathogenicity of poliovirus. J. Virol. **79:**4460–4469.
27. **Jackson, C. A., C. Cobbs, J. D. Peduzzi, M. Novak, and C. D. Morrow.** 2001. Repetitive intrathecal injections of poliovirus replicons result in gene expression in neurons of the central nervous system without pathogenesis. Hum. Gene Ther. **12:**1827–1841.
28. **Karber, G.** 1931. Beitrag zur kollektiven Behandlung pharmakologischer Reihenversuche. Arch. Exp. Pathol. Pharm. **162:**480.
29. **Kataoka, S., J. Satoh, H. Fujiya, T. Toyota, R. Suzuki, K. Itoh, and K. Kumagai.** 1983. Immunologic aspects of the nonobese diabetic (NOD) mouse. Abnormalities of cellular immunity. Diabetes **32:**247–253.
30. **Kauder, S. E., and V. R. Racaniello.** 2004. Poliovirus tropism and attenuation are determined after internal ribosome entry. J. Clin. Investig. **113:**1743–1753.
31. **Kawamura, N., M. Kohara, S. Abe, T. Komatsu, K. Tago, M. Arita, and A. Nomoto.** 1989. Determinants in the 5′ noncoding region of poliovirus Sabin 1 RNA that influence the attenuation phenotype. J. Virol. **63:**1302–1309.
32. **Kew, O. M., R. W. Sutter, E. M. de Gourville, W. R. Dowdle, and M. A. Pallansch.** 2005. Vaccine-derived polioviruses and the endgame strategy for global polio eradication. Annu. Rev. Microbiol. **59:**587–635.
33. **Kirchgessner, C. U., C. K. Patil, J. W. Evans, C. A. Cuomo, L. M. Fried, T. Carter, M. A. Oettinger, and J. M. Brown.** 1995. DNA-dependent kinase (p350) as a candidate gene for the murine SCID defect. Science **267:**1178–1183.
34. **Koike, S., H. Horie, I. Ise, A. Okitsu, M. Yoshida, N. Iizuka, K. Takeuchi, T. Takegami, and A. Nomoto.** 1990. The poliovirus receptor protein is produced both as membrane-bound and secreted forms. EMBO J. **9:**3217–3224.
35. **Koike, S., C. Taya, T. Kurata, S. Abe, I. Ise, H. Yonekawa, and A. Nomoto.** 1991. Transgenic mice susceptible to poliovirus. Proc. Natl. Acad. Sci. USA **88:**951–955.
36. **Komatsu, H., Y. Shimizu, Y. Takeuchi, H. Ishiko, and H. Takada.** 1999. Outbreak of severe neurologic involvement associated with enterovirus 71 infection. Pediatr. Neurol. **20:**17–23.
37. **La Monica, N., J. W. Almond, and V. R. Racaniello.** 1987. A mouse model for poliovirus neurovirulence identifies mutations that attenuate the virus for humans. J. Virol. **61:**2917–2920.
38. **Liu, C. C., W. C. Lian, M. Butler, and S. C. Wu.** 2007. High immunogenic enterovirus 71 strain and its production using serum-free microcarrier Vero cell culture. Vaccine **25:**19–24.
39. **Liu, M. L., Y. P. Lee, Y. F. Wang, H. Y. Lei, C. C. Liu, S. M. Wang, I. J. Su, J. R. Wang, T. M. Yeh, S. H. Chen, and C. K. Yu.** 2005. Type I interferons protect mice against enterovirus 71 infection. J. Gen. Virol. **86:**3263–3269.
40. **Lum, L. C., K. T. Wong, S. K. Lam, K. B. Chua, A. Y. Goh, W. L. Lim, B. B. Ong, G. Paul, S. AbuBakar, and M. Lambert.** 1998. Fatal enterovirus 71 encephalomyelitis. J. Pediatr. **133:**795–798.
41. **Martin, A., D. Benichou, T. Couderc, J. M. Hogle, C. Wychowski, S. Van der Werf, and M. Girard.** 1991. Use of type 1/type 2 chimeric polioviruses to study determinants of poliovirus type 1 neurovirulence in a mouse model. Virology **180:**648–658.
42. **Martin, A., C. Wychowski, T. Couderc, R. Crainic, J. Hogle, and M. Girard.** 1988. Engineering a poliovirus type 2 antigenic site on a type 1 capsid results in a chimaeric virus which is neurovirulent for mice. EMBO J. **7:**2839–2847.
43. **McGoldrick, A., A. J. Macadam, G. Dunn, A. Rowe, J. Burlison, P. D. Minor, J. Meredith, D. J. Evans, and J. W. Almond.** 1995. Role of mutations G-480 and C-6203 in the attenuation phenotype of Sabin type 1 poliovirus. J. Virol. **69:**7601–7605.
44. **McMinn, P. C.** 2002. An overview of the evolution of enterovirus 71 and its clinical and public health significance. FEMS Microbiol. Rev. **26:**91–107.
45. **Mendelsohn, C. L., E. Wimmer, and V. R. Racaniello.** 1989. Cellular receptor for poliovirus: molecular cloning, nucleotide sequence, and expression of a new member of the immunoglobulin superfamily. Cell **56:**855–865.
46. **Minor, P. D.** 1992. The molecular biology of polio vaccines. J. Gen. Virol. **73:**3065–3077.
47. **Murray, M. G., J. Bradley, X. F. Yang, E. Wimmer, E. G. Moss, and V. R. Racaniello.** 1988. Poliovirus host range is determined by a short amino acid sequence in neutralization antigenic site I. Science **241:**213–215.
48. **Nagata, N., T. Iwasaki, Y. Ami, A. Harashima, I. Hatano, Y. Suzaki, K. Yoshii, T. Yoshii, A. Nomoto, and T. Kurata.** 2001. Comparison of neuropathogenicity of poliovirus type 3 in transgenic mice bearing the poliovirus receptor gene and cynomolgus monkeys. Vaccine **19:**3201–3208.
49. **Nagata, N., T. Iwasaki, Y. Ami, Y. Tano, A. Harashima, Y. Suzaki, Y. Sato, H. Hasegawa, T. Sata, T. Miyamura, and H. Shimizu.** 2004. Differential localization of neurons susceptible to enterovirus 71 and poliovirus type 1 in the central nervous system of cynomolgus monkeys after intravenous inoculation. J. Gen. Virol. **85:**2981–2989.
50. **Nagata, N., H. Shimizu, Y. Ami, Y. Tano, A. Harashima, Y. Suzaki, Y. Sato, T. Miyamura, T. Sata, and T. Iwasaki.** 2002. Pyramidal and extrapyramidal involvement in experimental infection of cynomolgus monkeys with enterovirus 71. J. Med. Virol. **67:**207–216.
51. **Nijhuis, M., N. van Maarseveen, R. Schuurman, S. Verkuijlen, M. de Vos, K. Hendriksen, and A. M. van Loon.** 2002. Rapid and sensitive routine detection of all members of the genus enterovirus in different clinical specimens by real-time PCR. J. Clin. Microbiol. **40:**3666–3670.
52. **Omata, T., M. Kohara, S. Kuge, T. Komatsu, S. Abe, B. L. Semler, A. Kameda, H. Itoh, M. Arita, E. Wimmer, and A. Nomoto.** 1986. Genetic analysis of the attenuation phenotype of poliovirus type 1. J. Virol. **58:**348–358.
53. **Paul, A. V., J. Mugavero, J. Yin, S. Hobson, S. Schultz, J. H. van Boom, and E. Wimmer.** 2000. Studies on the attenuation phenotype of polio vaccines: poliovirus RNA polymerase derived from Sabin type 1 sequence is temperature sensitive in the uridylylation of VPg. Virology **272:**72–84.
54. **Pulli, T., P. Koskimies, and T. Hyypia.** 1995. Molecular comparison of coxsackie A virus serotypes. Virology **212:**30–38.
55. **Ren, R. B., F. Costantini, E. J. Gorgacz, J. J. Lee, and V. R. Racaniello.** 1990. Transgenic mice expressing a human poliovirus receptor: a new model for poliomyelitis. Cell **63:**353–362.
56. **Ren, R. B., E. G. Moss, and V. R. Racaniello.** 1991. Identification of two determinants that attenuate vaccine-related type 2 poliovirus. J. Virol. **65:**1377–1382.
57. **Rezapkin, G. V., L. Fan, D. M. Asher, M. R. Fibi, E. M. Dragunsky, and K. M. Chumakov.** 1999. Mutations in Sabin 2 strain of poliovirus and stability of attenuation phenotype. Virology **258:**152–160.
58. **Sabin, A. B.** 1965. Oral poliovirus vaccine. History of its development and prospects for eradication of poliomyelitis. JAMA **194:**872–876.
59. **Sambrook, J., and D. W. Russell.** 2001. Molecular cloning: a laboratory manual, 3rd ed., p 13.19–13.25. Cold Spring Harbor Laboratory Press, Cold Spring Harbor, NY.
60. **Schmidt, N. J., E. H. Lennette, and H. H. Ho.** 1974. An apparently new enterovirus isolated from patients with disease of the central nervous system. J. Infect. Dis. **129:**304–309.
61. **Shih, S. R., M. C. Tsai, S. N. Tseng, K. F. Won, K. S. Shia, W. T. Li, J. H. Chern, G. W. Chen, C. C. Lee, Y. C. Lee, K. C. Peng, and Y. S. Chao.** 2004. Mutation in enterovirus 71 capsid protein VP1 confers resistance to the inhibitory effects of pyridyl imidazolidinone. Antimicrob. Agents Chemother. **48:**3523–3529.
62. **Shiroki, K., T. Ishii, T. Aoki, Y. Ota, W. X. Yang, T. Komatsu, Y. Ami, M. Arita, S. Abe, S. Hashizume, and A. Nomoto.** 1997. Host range phenotype induced by mutations in the internal ribosomal entry site of poliovirus RNA. J. Virol. **71:**1–8.
63. **Smyth, M., J. Tate, E. Hoey, C. Lyons, S. Martin, and D. Stuart.** 1995. Implications for viral uncoating from the structure of bovine enterovirus. Nat. Struct. Biol. **2:**224–231.
64. **Tan, C. S., and M. J. Cardosa.** 2007. High-titred neutralizing antibodies to human enterovirus 71 preferentially bind to the N-terminal portion of the capsid protein VP1. Arch. Virol. **152:**1069–1073.
65. **Tardy-Panit, M., B. Blondel, A. Martin, F. Tekaia, F. Horaud, and F. Delpeyroux.** 1993. A mutation in the RNA polymerase of poliovirus type 1 contributes to attenuation in mice. J. Virol. **67:**4630–4638.
66. **Tung, W. S., S. A. Bakar, Z. Sekawi, and R. Rosli.** 2007. DNA vaccine

constructs against enterovirus 71 elicit immune response in mice. Genet. Vaccines Ther. **5:**6.

67. **Utagawa, E. T., E. Nakazawa, K. Matsuo, I. Oishi, N. Takeda, and T. Miyamura.** 2002. Application of an automated specimen search system installed in a transmission electron microscope for the detection of caliciviruses in clinical specimens. J. Virol. Methods **100:**49–56.
68. **Wagner-Ballon, O., H. Chagraoui, E. Prina, M. Tulliez, G. Milon, H. Raslova, J. L. Villeval, W. Vainchenker, and S. Giraudier.** 2006. Monocyte/macrophage dysfunctions do not impair the promotion of myelofibrosis by high levels of thrombopoietin. J. Immunol. **176:**6425–6433.
69. **Wang, S. M., H. Y. Lei, K. J. Huang, J. M. Wu, J. R. Wang, C. K. Yu, I. J. Su, and C. C. Liu.** 2003. Pathogenesis of enterovirus 71 brainstem encephalitis in pediatric patients: roles of cytokines and cellular immune activation in patients with pulmonary edema. J. Infect. Dis. **188:**564–570.
70. **Wang, S. M., C. C. Liu, H. W. Tseng, J. R. Wang, C. C. Huang, Y. J. Chen, Y. J. Yang, S. J. Lin, and T. F. Yeh.** 1999. Clinical spectrum of enterovirus 71 infection in children in southern Taiwan, with an emphasis on neurological complications. Clin. Infect. Dis. **29:**184–190.
71. **Wang, Y. F., C. T. Chou, H. Y. Lei, C. C. Liu, S. M. Wang, J. J. Yan, I. J. Su, J. R. Wang, T. M. Yeh, S. H. Chen, and C. K. Yu.** 2004. A mouse-adapted enterovirus 71 strain causes neurological disease in mice after oral infection. J. Virol. **78:**7916–7924.
72. **Wu, T. C., Y. F. Wang, Y. P. Lee, J. R. Wang, C. C. Liu, S. M. Wang, H. Y. Lei, I. J. Su, and C. K. Yu.** 2007. Immunity to avirulent enterovirus 71 and coxsackie A16 virus protect against enterovirus 71 infection in mice. J. Virol. **81:**10310–10315.
73. **Yu, C. K., C. C. Chen, C. L. Chen, J. R. Wang, C. C. Liu, J. J. Yan, and I. J. Su.** 2000. Neutralizing antibody provided protection against enterovirus type 71 lethal challenge in neonatal mice. J. Biomed. Sci. **7:**523–528.